

Physical mechanisms of interface-mediated intervalley coupling in Si

A.L. Saraiva,¹ M.J. Calderón,² Xuedong Hu,³ S. Das Sarma,⁴ and Belita Koiller¹

¹*Instituto de Física, Universidade Federal do Rio de Janeiro,
Caixa Postal 68528, 21941-972 Rio de Janeiro, Brazil*

²*Instituto de Ciencia de Materiales de Madrid (CSIC), Cantoblanco, 28049 Madrid, Spain*

³*Department of Physics, University at Buffalo, SUNY, Buffalo, NY 14260-1500*

⁴*Condensed Matter Theory Center, Department of Physics,
University of Maryland, College Park, MD 20742-4111*

(Dated: May 29, 2019)

The conduction band degeneracy in Si (valley-degeneracy) is known to be detrimental to spin quantum computing, for which nondegenerate ground orbital state is required. This degeneracy is lifted at an interface with an insulator, as the spatially abrupt change in the conduction band minimum leads to inter-valley scattering. We present an effective mass study of the interface-induced valley splitting in Si that provides simple criteria for optimal fabrication related conditions to maximize this splitting. Our work emphasizes the specific role played by the interface width in the quantitative determination of the valley splitting.

PACS numbers: 03.67.Lx, 85.30.-z, 85.35.Gv, 71.55.Cn

Semiconductor nanostructures based on GaAs and Si are approaching the limit where device functionality relies on degrees of freedom of individual electrons bound to a quantum dot [1] or to a donor [2]. Recent progress in material processing allows precisely controlled doping, band-structure engineering, and fabrication of high quality heterojunctions, which in turn pave the way for challenging applications such as the development of a scalable solid state quantum computer. Spin-based semiconductor quantum computer architectures were proposed more than 10 years ago [3]. The past few years witnessed tremendous experimental progress in the study of quantum dot spin qubit at the GaAs/AlGaAs interface [1], which raises an intriguing question on the feasibility of quantum computation in Si quantum dot [4] or donor states [5] at a Si/barrier-material interface.

A clear advantage of spin qubits in Si over GaAs is the long spin coherence times in Si [6]. On the other hand bulk Si conduction band edge is six-fold degenerate, a complication not present in GaAs. Near a (001) interface with a barrier material, this degeneracy is partially lifted, with the interface electron ground state remaining doubly degenerate. For electron spin qubits, the residual orbital degeneracy is an important spin decoherence source [7]. This effect can be overcome if the ground state double degeneracy is significantly lifted, which occurs close to an interface that can efficiently scatter carriers between the two degenerate valleys that are near opposite ends of the Brillouin zone [8]. Measurements of the doublet splitting, or valley splitting, present significant variations among different Si/barrier samples, ranging from 0 to ~ 1 meV [9]. In this context, a simple physical model that can help identify the relevant fabrication-related parameters in order to maximize the valley splitting is a valuable tool in assisting current experimental efforts.

Theoretical approaches to describe the electronic be-

havior in the presence of an interface or heterojunction range from the effective mass approximation (EMA) [10, 11], tight-binding models [12] to first-principles calculations [13]. Our study, based on the physically motivated EMA [14], aims to identify the relevance of sample-dependent parameters to the valley splitting. We study the effect of a single interface as a function of the conduction band-offset between (001) Si and the barrier material (barrier height) and the width of the interface. The full plane wave expansions of the Bloch functions at the two conduction band minima [15] involved contain relevant physical information about the underlying Si substrate, and are included explicitly. We identify favorable physical mechanisms and parameters that control the coupling strength pointing to convenient choices for the barrier material and the interface quality. We also highlight advantages and limitations of the EMA, in particular the oscillations of the valley coupling with the arbitrary choice of the interface position within a single monolayer (1 monolayer = $a_0/4$) distance [10], which is obviously an artifact of EMA.

We consider the (001) Si/barrier system, so that the 6-valley Si bulk degeneracy breaks into a 2-valley ground state and a 4-valley excited state quartet ~ 20 to 30 meV above the ground doublet [16]. We write the Hamiltonian for this problem as

$$H = H_0 + U(z) - \frac{F}{e}z, \quad (1)$$

where H_0 is the unperturbed bulk Si Hamiltonian. Translational symmetry is assumed in the xy plane, parallel to the interface, reducing the interface potential to a z -dependent profile $U(z)$. An electric field F along the z direction pushes the electron towards the interface. It is instructive to consider initially an abrupt interface between Si and the barrier material; we model it here by a

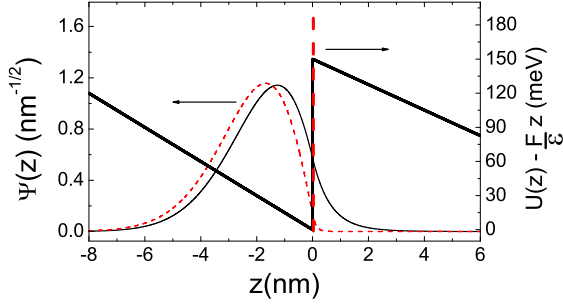


FIG. 1: Step model potential $U_{\text{step}}(z)$ (thick lines) and the calculated ground state envelope functions $\Psi(z)$ (thin lines) for the same electric field $F = 150$ kV/cm. The solid lines correspond to $U_0 = 150$ meV and dashed lines to $U_0 = 3$ eV, in which case the barrier potential is above the vertical scale of the figure. For any field value, the calculated valley splitting is defined by U_0 , $|\Psi(0)|^2$ and the evanescent tail $\Psi(z > 0)$.

simple step potential

$$U_{\text{step}}(z) = U_0 \Theta(z - z_I), \quad (2)$$

with U_0 representing the barrier height. The usual barrier material in Si devices are SiO_2 , corresponding to $U_0 \approx 3$ eV, and $\text{Si}_{1-x}\text{Ge}_x$ alloys, in which case U_0 depends on the alloy composition. A typical value, for $x \sim 0.2$ to 0.3 , would be $U_0 \approx 150$ meV.

Within single-valley EMA [14], the lowest energy conduction band eigenfunctions for Eq. (1) are written as $\phi_\mu(\mathbf{r}) = \Psi(z)e^{ik_\mu z}u_\mu(\mathbf{r})$ where $\mathbf{k}_\mu = \pm k_0 \hat{z}$ are the Bloch wave vectors of the conduction band minima ($k_0 \approx 0.84 \times 2\pi/a_0$). The envelope function $\Psi(z)$ satisfies the effective mass equation

$$\left\{ \frac{-\hbar^2}{2m_z} \frac{\partial^2}{\partial z^2} + U(z) - \frac{F}{\epsilon} z \right\} \Psi(z) = E \Psi(z), \quad (3)$$

where m_z is the longitudinal effective mass for Si. The ground state is numerically calculated through a finite differences method. Fig. 1 gives solutions obtained for $U_0 = 150$ meV and 3 eV under a 150 kV/cm applied field. Strictly within the EMA assumption that the perturbation potential varies slowly in the length scale of the lattice parameter a_0 , the ground state would remain doubly degenerate, since one obtains equivalent solutions for $\mathbf{k}_\mu = \pm k_0 \hat{z}$. This assumption is clearly not valid in the case of the step potential in Eq. (2) which is discontinuous at the interface position $z = z_I$, thus coupling the originally degenerate Bloch valley states $|\phi_\pm(\mathbf{r})\rangle$. Also, the electric field perturbation potential has a discontinuity in the derivative at $z = z_I$ due to the different values of the dielectric constant ϵ in the two materials. The interface position z_I is initially taken to be 0.

Since $\{|\phi_+\rangle, |\phi_-\rangle\}$ are well separated in energy from the excited states, an effective low energy Hamiltonian is

$$\bar{H} = \begin{pmatrix} E_0 & V_{VO} \\ V_{VO}^* & E_0 \end{pmatrix}, \quad (4)$$

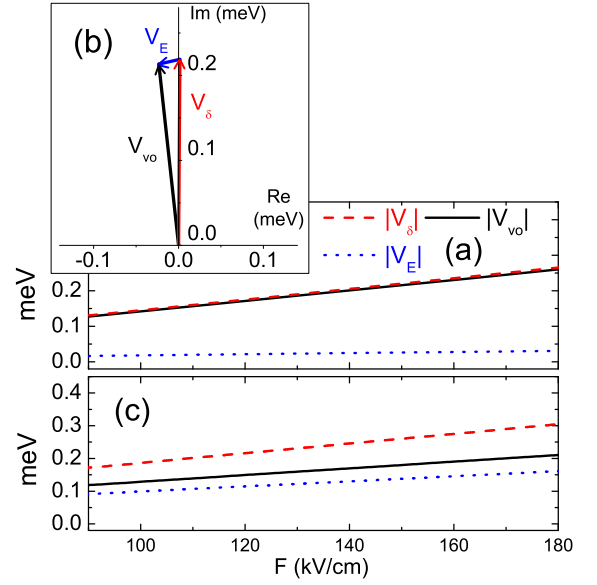


FIG. 2: (a) Absolute value of the intervalley coupling as a function of the electric field intensity for $U_0 = 150$ meV. The absolute values of the relevant terms in Eq. (8) are also shown. (b) Geometric representation of $V_{VO} = V_\delta + V_E$ in the complex plane for $U_0 = 150$ meV and $F = 150$ kV/cm. Although V_E does not affect $|V_{VO}|$ much, it rotates V_{VO} (i.e., changes its phase). (c) Same as frame (a) for $U_0 = 3$ eV.

where E_0 is the ground state energy obtained directly from Eq. (3), and the coupling due to the perturbation lifts the degeneracy leading to the valley splitting $2|V_{VO}|$. The quantity of interest determining the splitting is V_{VO} , also called valley-orbit coupling, given here by $V_{VO} = \langle \phi_+ | H | \phi_- \rangle$, which is a complex number. Note that H_0 gives no contribution to this coupling. We write the periodic functions u_\pm in terms of plane waves [15]

$$\phi_\pm = \Psi(z)e^{\pm ik_0 z} \sum_{\mathbf{G}} c_\pm(\mathbf{G})e^{i\mathbf{G} \cdot \mathbf{r}}, \quad (5)$$

taking \mathbf{G} to be the reciprocal lattice vectors. The expression for V_{VO} then reads

$$V_{VO} = \sum_{\mathbf{G}, \mathbf{G}'} c_+^*(\mathbf{G}) c_- (\mathbf{G}') \delta(G_x - G'_x) \delta(G_y - G'_y) I(G_z, G'_z), \quad (6)$$

where the orthonormality of the x and y components is used, since there is no perturbation potential along these directions. The last term is an integral

$$I(G_z, G'_z) = \int_{-\infty}^{+\infty} |\Psi(z)|^2 e^{iQz} \left[U_0 \Theta(z) - \frac{F}{\epsilon} z \right] dz \quad (7)$$

with $Q = G_z - G'_z - 2k_0$. Terms with \mathbf{G} and/or $\mathbf{G}' \neq 0$ contribute to the expression in Eq. (6) with values comparable to the $\mathbf{G} = \mathbf{G}' = 0$ term alone. Integrating the contribution of the step potential by parts, Eq. (6) is rewritten as

$$V_{VO} = V_\delta + V_E + V_F. \quad (8)$$

Here, V_δ is the contribution from the $I(G_z, G'_z)$ of the form $\frac{iU_0}{Q} \int_{-\infty}^{\infty} e^{iQz} |\Psi(z)|^2 \delta(z) dz = i\frac{U_0}{Q} |\Psi(0)|^2$, similar to the effect of a Q -dependent δ function coupling potential. The contributions to V_E , of the form $\frac{iU_0}{Q} \int_0^{\infty} e^{iQz} \frac{d|\Psi(z)|^2}{dz} dz$, involve only the evanescent part of the envelope function penetrating into the barrier region. We find V_F , the electric field potential contribution, to be negligible in all cases considered here, meaning that the “kink” in the electric field potential at the interface is not singular enough to couple the $|\phi_\pm\rangle$, thus following the standard EMA assumption. The main effect of the field is to confine the electron near the surface, and it is clear that the envelope function changes with F .

Fig. 2(a) shows the absolute value of the coupling, $|V_{VO}|$ and of the $|V_\delta|$ and $|V_E|$ terms, for $U_0 = 150$ meV, as a function of applied field. In this case $|V_{VO}|$ is well described by the δ -function contributions alone. If one is also interested in the eigenstates, the phase in V_{VO} becomes relevant and the contribution V_E plays a role, as illustrated in Fig. 2(b). Fig. 2 (c) gives the results for the couplings dependence on the field for $U_0 = 3$ eV, and in this case both contributions affect $|V_{VO}|$. For all values of U_0 , the coupling increases monotonously with the field, with an approximately linear behavior at larger fields [8, 10, 12].

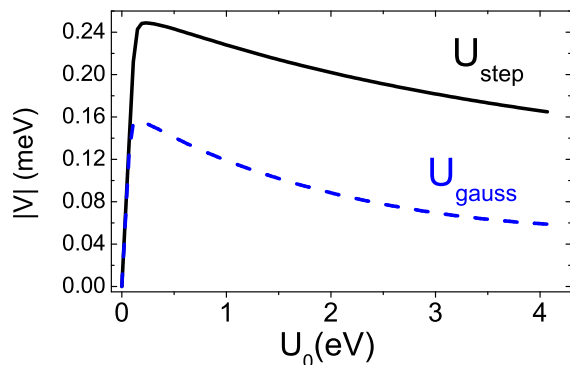


FIG. 3: Variation of the absolute value of the valley orbit coupling with barrier height for $F = 150$ kV/cm. The step model of Eq. (2) and the smeared ($L = 1$ monolayer) profile of Eq. (10) are shown as the solid and dashed lines respectively. Both present a maximum for $U_0 \approx 200$ meV.

The expression for V_δ indicates that it is proportional to the product $U_0 |\Psi(0)|^2$. As U_0 increases, $|\Psi(0)|^2$ decreases, so maximizing $|V_\delta|$ involves particular and not obvious conditions. The same is true for V_E , for which only the evanescent tail ($z > 0$) of $\Psi(z)$ contributes. As shown in Fig. 1, when U_0 decreases the z -range that makes significant contribution to the integration increases. However, the highly oscillatory phases e^{iQz} in the integrand usually suppresses this contribution. Nevertheless, a comparison of Fig. 2(a) and (c) shows that the larger U_0 actually produces a much larger $|V_E|$, even though it corresponds to a more rapidly decaying evanes-

cent envelope. Maximizing $|V_\delta|$ and $|V_E|$ independently does not necessarily maximize the absolute value of the complex sum $V_\delta + V_E = V_{VO}$. The net result is that $|V_{VO}|$ may be similar in magnitude even for materials with U_0 a factor of 20 apart, as shown in Fig. 2. The general behavior of $|V_{VO}|$ with the barrier height U_0 is illustrated in Fig. 3 (solid line) for $F = 150$ kV/cm. As U_0 increases from 0, a sharp rise in $|V_{VO}|$ is obtained up to a maximum coupling value around $U_0 \approx 200$ meV, followed by a slow decay: Very low or very high barriers tend to suppress the valley coupling. Tuning U_0 involves changing the alloy composition in the barrier, as in the case of $\text{Si}_{1-x}\text{Ge}_x$, or changing the barrier material. Such fabrication processes are not straightforward, but are in principle experimentally feasible.

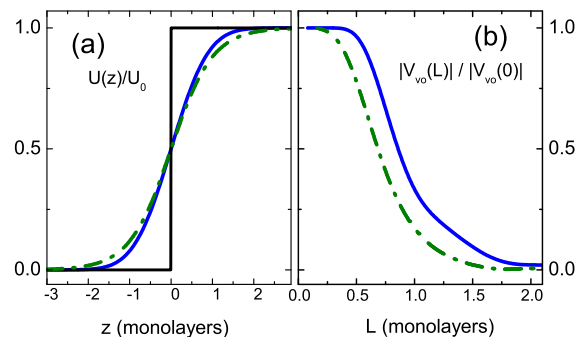


FIG. 4: (a) Normalized potential profiles for the finite-width interface models [Eqs. (9) and (10)]. The step potential is also given. For U_{gauss} (solid curve) and U_{exp} (dashed curve) the same width $L = 1$ monolayer is taken. (b) Variation with the interface width L of the normalized valley coupling for $F=150$ kV/cm and $U_0 = 150$ meV. The step potential corresponds to $L = 0$ in both models. Reported sample measurements are consistent with $L \approx 1 - 2$ monolayers. Note that the slightly steeper U_{gauss} significantly increases $|V_{VO}|$.

We now consider the effect of the interface width [17], which is disregarded in the step model. We use interface models that are similar to previously measured and calculated profiles [18], namely

$$U_{\text{exp}}(z) = \frac{U_0}{2} [\tanh(z/L) + 1], \quad (9)$$

$$U_{\text{gauss}}(z) = \frac{U_0}{2} \text{Erfc}(-z/L), \quad (10)$$

where $\text{Erfc}(x)$ is the complementary error function. Both are characterized by a width L , and reproduce $U_{\text{step}}(z)$ for $L = 0$. They differ in the asymptotic behavior (respectively exponential and gaussian). The two forms are compared in Fig. 4(a) for $L = 1$ monolayer. The curves are very similar, as quantified by the RMS deviation with respect to the step potential; the U_{exp} RMS is only 8% larger than that of the U_{gauss} profile. Yet, values of $|V_{VO}|$ differ by a factor of two. This factor may be as large as

3 (for $L \approx 1.3$) with the same RMS ratio between the profiles. Fig. 4(b) gives the calculated coupling versus L .

The interface width tends to suppress the intervalley coupling, as illustrated by the dashed lines in Fig. 3. Indeed, when L goes beyond a couple of monolayers, the intervalley coupling $|V_{VO}|$ almost completely vanishes. The sensitivity of the coupling to the particular functional form of the interface potential for the same value of L indicates that in real samples the coupling is strongly dependent on the type of interface disorder and roughness, in addition to its width. Both effects contribute to the experimentally observed highly sensitive sample dependence of the intervalley scattering.

A fundamental limitation of the step potential is the sensitivity of the results to the interface position z_I (taken to be 0 in the results presented so far) on a sub-monolayer length scale. This artifact, already obtained by Sham and Nakayama [10], is due to the periodic parts of the Bloch functions, which carry information about the underlying Si lattice and lead to different interference patterns due to the interface perturbation according to its location. Results for $|V_{VO}|$ as a function of z_I for the step potential are given by the triangles in Fig. 5. As expected, $|V_{VO}|$ shows oscillatory behavior with a 1 monolayer period, but different models lead to different relative phases. The more physical model with a finite interface width partially overcomes this artifact, as the amplitude of the oscillations is reduced for finite L . This is illustrated by the squares in Fig. 5, and leads us to believe that a realistic model of the interface would largely, if not completely, remove this sensitivity to the exact interface location.

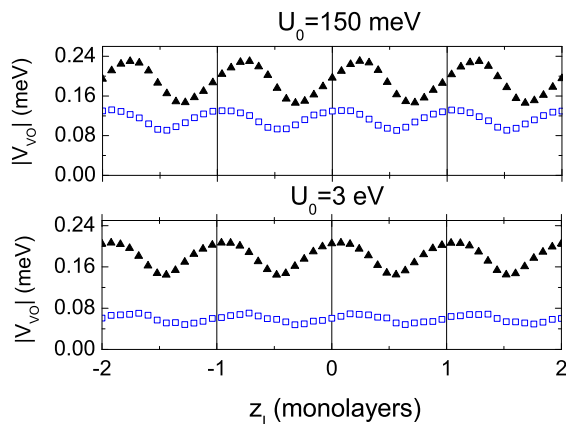


FIG. 5: Dependence of the intervalley coupling on the positioning of the interface profile relative to the lattice atomic positions for $U_0 = 150$ meV and 3 eV. The triangles represent U_{step} [Eq.(2)] and squares U_{gauss} [Eq.(10)], with $L = 1$ monolayer.

In summary, we have studied the conduction electron valley splitting in Si at a *single* Si/barrier interface using EMA. For a sharp interface, the simplicity of EMA

allows us to identify two main contributions to the valley splitting: the electron wave function at the interface and the wave function gradient for the evanescent wave in the barrier material. We show that an external field (to increase the wave function at the interface) and an appropriate barrier potential height (through proper alloying or choice of barrier material) can help maximize the valley splitting.

A shortcoming of the sharp interface model is that its results are highly sensitive to the location of the interface. We remedy this deficiency by introducing a finite width to the interface. The finite width reduces the sensitivity to the interface location while also reducing the intervalley scattering, because it blunts the sharp intervalley interference. This is illustrated by our result that steeper interfaces always favor larger inter-valley splitting.

We do not expect our EMA results to be quantitatively accurate. Many effects are not explicitly included, such as strain, interface misorientation, atomic scale fluctuations, and lateral profiles of the interface and confinement. We also do not include any many-body corrections to the valley splitting. Nonetheless, the splittings $2|V_{VO}|$ on the order of 0.5 meV we calculated are in fair agreement with available measurements in Si/SiO₂ and Si/SiGe interfaces regarding the intrinsic interface contribution.

In conclusion, we have calculated electron valley splitting in Si at a Si/barrier interface. We show that a single-particle valley splitting in the order of 0.5 meV can be generated by applying a proper external field, choosing an optimal barrier material of a suitable potential height, and producing a high quality sharp interface. Lateral confinement of the electron and many-body corrections can potentially further increase the valley splitting.

This work was partially supported by the Brazilian agencies CNPq, FUB, Millenium Institute on Nanotechnology - MCT, and FAPERJ. MJC acknowledges MAT2006-03741 and the Ramón y Cajal program (MICINN, Spain). XH and SDS thank financial support by NSA and LPS through US ARO, and by NSF.

-
- [1] R. Hanson, L. P. Kouwenhoven, J. R. Petta, S. Tarucha, and L. M. K. Vandersypen, *Rev. Mod. Phys.* **79**, 1217 (2007).
 - [2] G. P. Lansbergen, R. Rahman, C. J. Wellard, J. C. I. Woo, N. Collaert, S. Biesemans, G. Klimeck, L. C. L. Hollenberg, and S. Rogge, *Nat. Phys.* **4**, 656 (2008).
 - [3] D. Loss and D. P. DiVincenzo, *Phys. Rev. A* **57**, 120 (1998); B. E. Kane, *Nature* **393**, 133 (1998).
 - [4] M. Friesen, P. Rugheimer, D. E. Savage, M. G. Legally, D. W. van der Weide, R. Joynt, and M. A. Eriksson, *Phys. Rev. B* **67**, 121301 (2003).
 - [5] M. J. Calderón, B. Koiller, X. Hu, and S. Das Sarma, *Phys. Rev. Lett.* **96**, 096802 (2006).

- [6] S. Das Sarma, R. de Sousa, X. Hu, and B. Koiller, Solid State Commun. **133**, 737 (2004).
- [7] C. Tahan, M. Friesen, and R. Joynt, Phys. Rev. B **66**, 035314 (2002).
- [8] T. Ando, A. Fowler, and F. Stern, Rev. Mod. Phys. **54**, 437 (1982).
- [9] K. Takashina, A. Fujiwara, S. Horiguchi, Y. Takahashi and Y. Hirayama, Phys. Rev. B **69**, 161304 (2004); S. Goswami, K. A. Slinker, M. Friesen, L. M. McGuire, J. L. Truitt, C. Tahan, L. J. Klein, J. O. Chu, P. M. Mooney, D. W. van der Weide, R. Joynt, S. N. Coppersmith, M. A. Eriksson, Nat. Phys. **3**, 41 (2007).
- [10] L. Sham and M. Nakayama, Phys. Rev. B **20**, 734 (1979).
- [11] M. Friesen, S. Chutia, C. Tahan, and S. N. Coppersmith, Phys. Rev. B **75**, 115318 (2007).
- [12] G. Grosso, G. P. Parravicini, C. Piermarocchi, Phys. Rev. B **54**, 16393 (1996); T. B. Boykin, G. Klimeck, M. Friesen, S. N. Coppersmith, P. von Allmen, F. Oyafuso and S. Lee, Phys. Rev. B **70**, 165325 (2004).
- [13] B. A. Foreman, Phys. Rev. B **72**, 165345 (2005).
- [14] W. Kohn, *Solid State Physics Series*, vol. 5 (Academic Press, 1957), edited by F. Seitz and D. Turnbull.
- [15] B. Koiller, R. B. Capaz, X. Hu, and S. Das Sarma, Phys. Rev. B **70**, 115207 (2004).
- [16] B. E. Kane, Fortschr. Phys. **48**, 1023 (2000).
- [17] F. Stern, Solid State Commun. **21**, 163 (1977); T. Ishiyama, M. Nagase and Y. Omura, Appl. Surf. Sci. **190**, 16 (2002).
- [18] P. E. Batson, Journ. of Electron Microscopy **49**, 267 (2000); T. Yamasaki, C. Kaneta, T. Uchiyama, T. Uda and K. Terakura, Phys. Rev. B **63**, 115314 (2001).